Pseudospin valve in bilayer graphene nanoribbons

Xiaoguang Li,[1] Zhenyu Zhang,[1,2,3] and Di Xiao[2]
[1]*Department of Physics and Astronomy, The University of Tennessee, Knoxville, Tennessee 37996, USA*
[2]*Materials Science and Technology Division, Oak Ridge National Laboratory, Oak Ridge, Tennessee 37831, USA*
[3]*ICQD, University of Science and Technology of China, Hefei, Anhui, China*
(Received 2 February 2010; published 3 May 2010)

We study the pseudospin valve effect in bilayer graphene nanoribbons using the recursive Green's function method. The pseudospin degree of freedom is associated with the electron density in two layers and can be controlled by external gate electrodes. We find that the conductance of nanoribbons shows different behavior compared to infinite systems due to the appearance of edge states and quantum confinement. Remarkably, a large on-off ratio can be achieved in nanoribbons with zigzag edges, even when the Fermi energy lies in the bulk energy gap. The influence of possible edge vacancies and interface conditions is also discussed.

DOI: 10.1103/PhysRevB.81.195402 PACS number(s): 72.80.Vp, 73.23.Ad, 73.40.−c, 73.63.−b

I. INTRODUCTION

Recent years have seen a surge of interest in graphene materials,[1–3] motivated by their potential application as a building block in future nanoelectronics.[4] Unlike conventional semiconductors, the charge carriers in graphene are described by a two-dimensional Dirac-like equation[5,6] and display gigantic intrinsic mobility even at room temperature.[7–9] These unique properties are responsible for a slew of spectacular phenomena such as the half-integer quantum Hall effect[10–13] and Klein tunneling.[6] However, they also make it extremely difficult to manipulate the current-conducting state in graphene-based circuits. Among various schemes proposed to deal with this problem, a common solution is to induce a band gap in the energy spectrum by, for example, chemical doping in the bulk[14] or quantum size effect in nanoribbons.[15]

More recently, there has been an increasing interest in bilayer graphene[16–32] because they allow easy tuning of the band structure via gate electrodes,[33–37] which, in turn, provides a promising avenue toward controlled transport in graphene-based circuits. The honeycomb lattice of a monolayer graphene consists of two atoms in a unit cell, conventionally labeled by A and B atoms. In bilayer graphene, the two layers are typically stacked in the so-called Bernard form in which an A atom of the top layer sits right above a B atom of the bottom layer (Fig. 1). Therefore, applying an electric field perpendicular to the layers will break the sublattice symmetry of the system and open a band gap. Experimentally, it has been demonstrated that the band gap can be tuned up to 250 meV,[37] well into the midinfrared frequency range.

In addition, bilayer graphene also possess a pseudospin degree of freedom associated with the electron-density difference between the two layers.[38–40] The aforementioned perpendicular electric field plays the role as a "Zeeman" field that couples to the pseudospin. Based on this analogy, San-Jose *et al.*[40] recently proposed a pseudospin valve (PSV) device that consists of a bilayer graphene with a pair of adjacent gate electrodes. This device operates in a similar way as the spin valve,[41] i.e., by changing the polarity of the gate voltage, parallel and antiparallel pseudospin configurations can be realized and the device can be switched between on and off states. It has been shown that a large on-off ratio of the conductance can be achieved when the Fermi energy lies just outside the bulk band gap.

The issue to be addressed in this paper is the effect of confined geometry, particularly the appearance of the edge states, on the PSV. Graphene materials are known to have edge states on zigzag edges,[42,43] which can significantly affect the transport properties of the system.[44,45] Here we demonstrate by numerical simulations that a "midgap" PSV effect exists in bilayer graphene nanoribbons, in which the device can operate with a large on-off ratio even when the Fermi energy is inside the bulk band gap. This effect is possible because in addition to the flat-band edge states typically found in monolayer graphene, bilayer graphene also has edge states that are dispersive and extend well into the bulk band gap.[46] These are the states that carry currents when the bulk states are not available. Moreover, due to the nonlocalized property of these edge states, the midgap PSV effect is robust against edge defects. Our result also shows that a smooth gate potential, as one is likely to encounter in real experiments, will have limited influence on the operation of this device. These features make PSV a highly desired method to

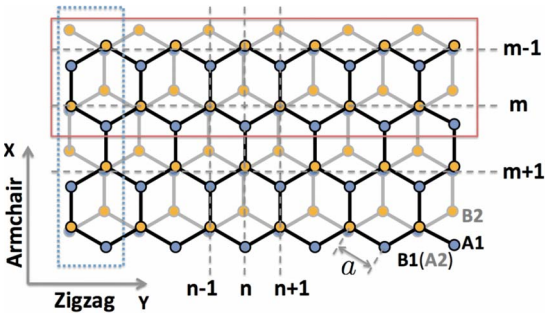

FIG. 1. (Color online) Geometry of bilayer graphene nanoribbon. Black bonds connect atoms in the top layer and gray bonds connect atoms in the bottom layer. The line in armchair direction is labeled with n and zigzag direction is labeled with m. An armchair nanoribbon with width N has $4N$ atoms in a principal layer (in red solid frame), and a zigzag nanoribbon width M has $4M$ atoms in a principal layer (in blue dot frame).

control electric currents in graphene-based circuits with confined geometry.

This paper is organized as follows. Section II describes the model system, especially the properties of the dispersive edge states in bilayer graphene nanoribbons. In Sec. III, conductance of both armchair and zigzag bilayer graphene nanoribbons is studied in detail by recursive Green's function method. We close the paper with a summary in Sec. IV.

II. MODEL

The bilayer graphene with a biased voltage between the two layers can be described by the tight-binding Hamiltonian[2,31]

$$H = \sum_{l=1,2;\langle i,j\rangle} (V^A_{l,i} a^\dagger_{l,i} a_{l,i} + V^B_{l,j} b^\dagger_{l,j} b_{l,j}) - t \sum_{l=1,2;\langle i,j\rangle} (a^\dagger_{l,i} b_{l,j} + \text{H.c.}) - t_\perp \sum_i (a^\dagger_{1,i} b_{2,i} + \text{H.c.}), \quad (1)$$

where l is the layer index and i,j label the unit cell within one layer. The operator $a_{l,i}(b_{l,j})$ annihilates an electron at the $A(B)$ site in the ith unit cell of layer l. $V^{A,B}_{l,i}$ is the site energy, which can be controlled by the biased voltage, t is the intralayer nearest-neighbor hopping ($\simeq 2.9$ eV), and $t_\perp$ is the interlayer hopping ($\simeq 0.39$ eV) between A_1 and B_2, as shown in Fig. 1.

In the presence of a uniform perpendicular electric field, the site energy $V^{A,B}_{l,i}$ is constant within one layer, i.e., $V^{A,B}_{l,i} = V_l$. Introduce the potential average $V_\mu = (V_1 + V_2)/2$ and the potential difference $V_0 = (V_1 - V_2)/2$. The energy spectrum of the system has a direct band gap of the size $2|V_0|$ at the two inequivalent corners, K and K', of the Brillouin zone. In experiments, one can change the Fermi energy (through V_μ) and the band gap (through V_0) at the same time by adjusting the gate voltages.[37]

The pseudospin degree of freedom is defined as the electron population difference between the two layers. To find its explicit dependence on the bias voltage, we recast Hamiltonian (1) in the momentum space and focus on the low-energy sector that governs the quasiparticle dynamics. The effective Hamiltonian around the K point reads

$$H = \begin{pmatrix} V_0 & v_F\pi^\dagger & 0 & 0 \\ v_F\pi & V_0 & t_\perp & 0 \\ 0 & t_\perp & -V_0 & v_F\pi^\dagger \\ 0 & 0 & v_F\pi & -V_0 \end{pmatrix}, \quad (2)$$

where $v_F = \frac{3}{2}at/\hbar$ with a being the lattice constant (we use units such that $\hbar = 1 = v_F$ from now on) and $\pi = p_x + ip_y$ is the momentum measured from the K point in the Brillouin zone. The Hamiltonian around the K' point can be obtained by replacing π with $p_x - ip_y$. We have dropped the V_μ term because it corresponds to a constant shift of all energy levels, or equivalently, a shift of the relative position of the Fermi energy E_F. For $|V_0| \ll t_\perp$, the Hamiltonian can be further reduced to,[13]

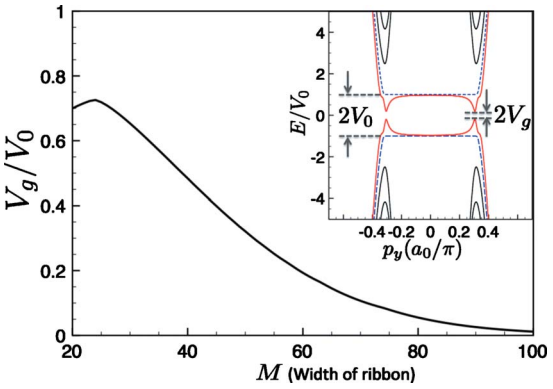

FIG. 2. (Color online) Energy gap between the dispersive edge states (red in the inset) in zigzag nanoribbons as a function of the nanoribbon width. Inset: the spectrum of a zigzag nanoribbon with width $M = 60$.

$$H \simeq \begin{pmatrix} V_0 & (\pi^\dagger)^2/t_\perp \\ (\pi)^2/t_\perp & -V_0 \end{pmatrix}. \quad (3)$$

The resulting two-component wave functions describe the electronic amplitudes on A_1 and B_2 sites. For a given eigenstate Ψ with energy E, the pseudospin is defined by

$$\langle\Psi|\boldsymbol{\sigma}|\Psi\rangle = \sqrt{1 - \left(\frac{V_0}{E}\right)^2}(\cos 2\theta_p \hat{x} + \sin 2\theta_p \hat{y}) + \frac{V_0}{E}\hat{z}, \quad (4)$$

where $\theta_p = \arctan(p_y/p_x)$. We can clearly see that the pseudospin can be tuned by the potential difference V_0.

The bulk PSV proposed by San-Jose *et al.*[40] consists of a pair of adjacent gate electrodes with tunable bias voltage. When the two gates have the same (opposite) potential difference, the electrons in two gated region have parallel (antiparallel) pseudospins. In the antiparallel configuration the transmission rate will be strongly suppressed because of the interface pseudospin flipping, while in the parallel configuration the pseudospin does not play a role. As a result, the system can be changed between on and off states.

Next we consider the energy spectrum of the bilayer graphene system described by Hamiltonian (1) in a confined geometry. In addition to the energy quantization, the most visible difference between the bulk and nanoribbon graphene systems is the appearance of the edge states.[2,46] Shown in the inset of Fig. 2 is the energy spectrum of the bilayer graphene with zigzag edges. We can see that in addition to the two flat-band-edge states, as usually seen in monolayer graphene, there are two more edge states with dispersive-energy bands. In bilayer graphene, there are four different edges terminated by atoms of the type $A1$, $B1$, $A2$, and $B2$, respectively (Fig. 1). The two flat-band-edge states are strictly localized on the edge atoms $A1$ and $B2$, separated by an energy gap of $2|V_0|$. On the other hand, due to the coupling $t_\perp$ between the two layers, the other two edge states (residing on the edges formed by atoms $B1$ and $A2$) are dispersive and can penetrate into the bulk.[46] Remarkably, the band structure of these edge states extends well into the bulk band gap ("midgap" region). Figure 2 shows the behavior of the small gap $2V_g$

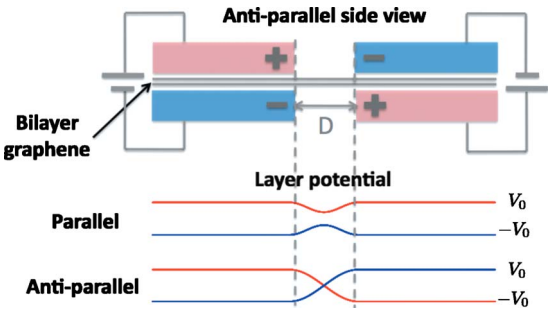

FIG. 3. (Color online) Electrode setup for antiparallel configuration and potential function of different configurations. The red (blue) line refers to top (bottom) layer potential.

between the dispersive edge states as a function of the nanoribbon width. It is clear that as the nanoribbon width increases, the dispersive edge states tend to extend to the whole midgap region and the energy spectrum becomes essentially gapless. This opens up the possibility of transport phenomena at an arbitrary Fermi energy.

The setup of the PSV is shown in Fig. 3 with an interface of length D connecting two semi-infinite gated regions. The transmission rate of electrons through the whole system is calculated using the standard recursive Green's function method,[47] which is a widely used technique in the study of transport properties.[31,40,48–58] Within this approach, the system is sliced into a series of principal layers (Fig. 1), and then the Green's function is calculated by propagating an initial function layer by layer from one end to the other. We use the algorithm developed by Sancho *et al.*[59] to mimic the semi-infinite leads by a finite region with a large number of principle layers. Finally, the conductance is calculated by the Landauer formula

$$G = \frac{2e^2}{h}T, \tag{5}$$

where T is the transmission rate obtained from the Green's function. The factor of 2 comes from the spin degeneracy.

III. RESULTS AND DISCUSSIONS

A. Conductance of bilayer nanoribbons

We first consider a bilayer graphene nanoribbon with an abrupt interface between the two gated regions. For antiparallel configuration, we have

$$V_0(x) = V_0[1 - 2\theta(x)], \tag{6}$$

and for parallel configuration, $V_0(x)$ is a constant. The interface length $D=0$.

The conductance of nanoribbons with armchair and zigzag edges is shown in Fig. 4. We immediately notice that, in sharp contrast to armchair edges, nanoribbons with zigzag edges have a finite conductance even when the Fermi energy is in the midgap region. Moreover, the conductance of the parallel and antiparallel configurations shows a sizable difference in this region, giving rise to a "midgap" PSV effect. To quantify the PSV effect, we define the pseudospin magnetoresistance (PMR) following Ref. 40

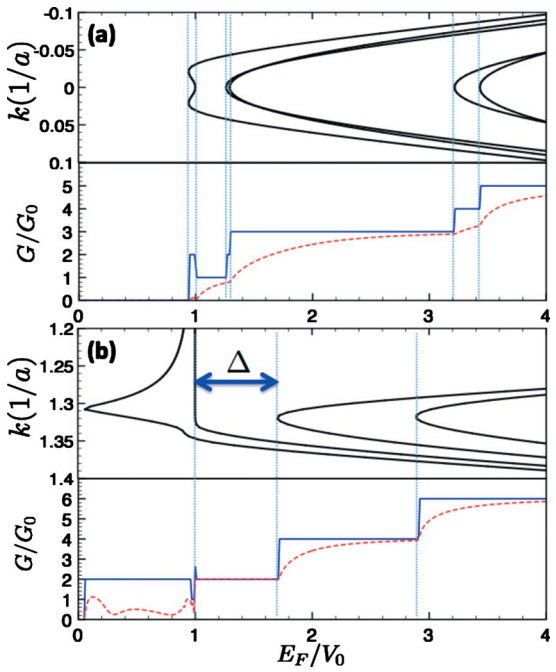

FIG. 4. (Color online) The band structure and conductance for bilayer graphene nanoribbons with (a) zigzag and (b) armchair edges. The width of both nanoribbons is 80. The blue solid line refers to parallel configuration and the red dashed line refers to antiparallel configuration. $V_0=70$ meV is the potential difference between the layers. $G_0=2e^2/\hbar$ is the unit conductance.

$$\mathrm{PMR} = \frac{G_P - G_{AP}}{G_P}, \tag{7}$$

where $G_P(G_{AP})$ is the conductance for parallel (antiparallel) configuration. The PMR for both edges is shown in Fig. 5.

To understand the behavior of the PMR we have also plotted the corresponding band structure in Fig. 4. For the antiparallel configuration the translational symmetry along the nanoribbon direction is broken because of the interface. Nonetheless we can still consider the *local* band structure inside the semi-infinite leads far way from the interface. The band structures with opposite V_0 are exactly the same. For

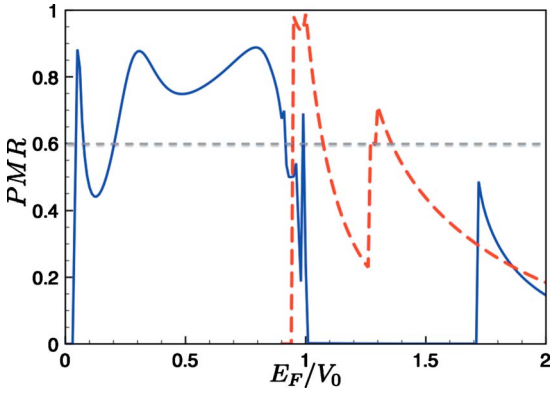

FIG. 5. (Color online) PMR for bilayer graphene nanoribbon with zigzag (blue solid) and armchair (red dashed) edges. The width of both nanoribbons is 80.

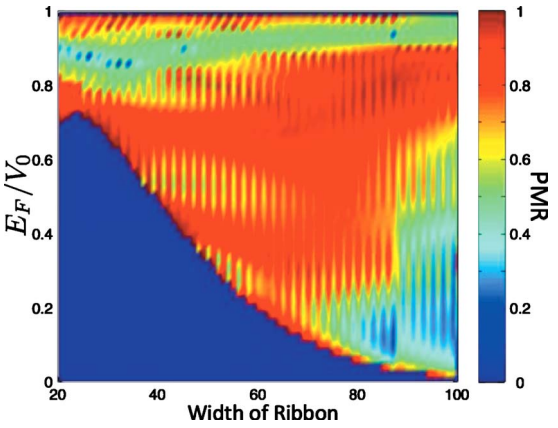

FIG. 6. (Color online) Fermi energy and width dependence of the PMR in zigzag nanoribbons.

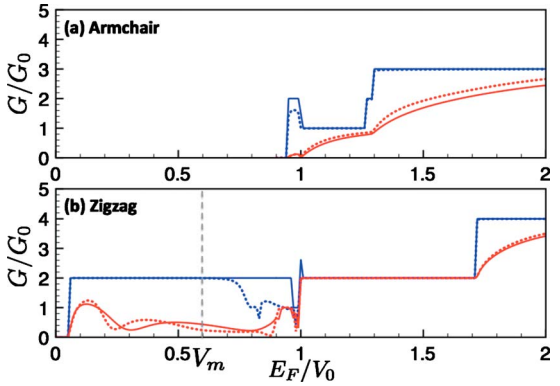

FIG. 7. (Color online) Conductance of (a) armchair ($N=80$) and (b) zigzag ($M=80$) nanoribbons. The solid lines refer to the idea abrupt potential change on the interface. The dashed lines refer to the smooth potential change with interface length of $D=5$ and $V_m=0.6V_0$ for parallel configuration. Red (blue) lines refer to parallel (antiparallel) configuration.

zigzag edges we only show one of the valleys because the intervalley scattering involves large momentum transfer and contributes little to the total conductance. By comparing the band structure of the zigzag and armchair nanoribbons, we can clearly see that the midgap PSV effect originates from the dispersive edge states discussed earlier. The efficiency of the midgap PSV is comparable to its bulk counterpart with a fairly large PMR in the bulk band gap ($>=60\%$).

Several remarks are in order. (i) For parallel configurations, the conductance shows a steplike behavior as a function of the Fermi energy, typical for finite-size system. On the other hand, for antiparallel configurations, the conductance varies much smoother, increasing gradually when the Fermi energy is between two subbands. This can be attributed to the fact that for a given energy band, the z component of the pseudospin has its largest value at the band bottom then decreases as the energy increases [see Eq. (4)]. (ii) The largest difference between G_P and G_{AP} is $2G_0$ at the subband bottom. As both G_P and G_{AP} increases with Fermi energy, the peak value of PMR decreases. (iii) We note that for zigzag nanoribbons, there exists a region [the Δ region[44,60] in Fig. 4(b)], where the PMR vanishes with equal G_P and G_{AP}. In this region, if the electrons are limited to one of the valleys then the backscattering is completely eliminated. The perfect transmission of the antiparallel configuration therefore indicates that the pseudospin flipping process happens at a much faster rate than the intervalley scattering. In other words, the electrons will experience a sudden pseudospin flipping without being scattered to the other valley.

Finally, to obtain a comprehensive picture of the conductance of edge states in the midgap region, we plot in Fig. 6 the Fermi-energy dependence of PMR for a zigzag nanoribbon with its width varying from 20 to 100. We can see that compared to the bulk PSV effect, in which the PMR is appreciable only in a small window of E_F, there is a wide parameter range where a large PMR can be archived for the midgap PSV effect.

B. Conductance with finite interface

Having demonstrated the midgap PSV effect for an ideal abrupt interface, next we discuss more realistic interface conditions. In a real experiment, the two external gates are usually separated by a certain distance and $V_0(x)$ should vary smoothly in space. Here, we consider a PSV with interface of length D. The origin of the x axis is chosen at the middle. The on-site potential is constant in the lead region and modeled by the following function in the central region:

$$V_1 = -V_2 = -V_0 \sin\left(\frac{\pi}{D}x\right) \tag{8}$$

for antiparallel configuration and

$$V_1 = -V_2 = \frac{V_0 + V_m}{2} - \frac{V_0 - V_m}{2}\cos\left(\frac{2\pi}{D}x\right) \tag{9}$$

for parallel configuration, where V_1 (V_2) is on-site potential of top (bottom) layer and $2V_m$ is the band-gap minimum in the central region for the parallel configuration. Both potential profiles are shown in Fig. 3. Here the parameter V_m is included to account for the fact that there may be a region in the middle uncovered by both gate electrodes (Fig. 3). When $V_m=V_0$, we recover the ideal situation discussed by San-Jose *et al.* in bulk PSV.[40] However, as we will show later, a nonzero V_m can have a strong effect on the PMR.

In Fig. 7, we compare the conductance of the PSV with a smooth interface to an abrupt interface for both armchair and zigzag nanoribbons. We can see that the conductance with finite interface tends to suppress the PSV effect for both armchair and zigzag nanoribbons. The general cause has been discussed by San-Jose *et al.*[40] in their bulk PSV study—with a large interface length D, electrons will have a long distance to adjust its pseudospin according to the profile of $V_0(x)$ and are able to pass through the interface by gradually accommodate the change instead of being reflected. Following this argument, we can see that the potential dip in the central region characterized by V_m can affect the conductance of parallel configuration. To understand this effect, let us consider an extreme case where $V_m=0$. Then even in parallel configuration the pseudospin need to be quickly rotated to in plane once the electrons are in the central region, be-

cause the pseudospin has no $\hat{z}$ component there. As a result, G_P is reduced and so does the PMR. There are, however, several additional features specific to the nanoribbon geometry. (i) The zero PMR region of the zigzag nanoribbons is unaffected at all, thanks to the absence of backscattering. (ii) The V_m term can significantly alter the edge state dispersion, therefore creating a large-momentum mismatch at the interface. This causes the large drop of G_P in the midgap region, as seen in Fig. 7(b).

Due to the crucial role of V_m for parallel configuration, it is much desired to make the interface length D small enough to ensure that V_m is close to V_0.

C. Edge disorder

In this section, we study the influence of edge disorder on the midgap PSV effect. Previous studies have shown that in both monolayer and bilayer graphene the edge disorder will strongly affect the conductance of both zigzag and armchair nanoribbons.[31,53,61] In our calculation, we again consider an abrupt interface. The system consists of two clean, semi-infinite leads on the two sides and a central region of 40 principle layers where the disorder occurs. The interface is placed in the middle of the central region. In one principle layer, vacancies can appear at four available positions for zigzag nanoribbons and eight available positions for armchair nanoribbons. In our tight-binding calculation the vacancy is simulated by setting the on-site energy to infinity.[51,53,62]

In Fig. 8, we show the comparison between a clean nanoribbon and one with edge disorder. For armchair nanoribbons, even a tiny amount of edge impurity (the impurity concentration $p=2.5\%$) makes the PSV highly unreliable. This can be seen in Fig. 8(c); the PMR can drop to below 20% when the Fermi energy is in the first subband. On the other hand, for zigzag nanoribbons, even with a higher impurity concentration ($p=10\%$) the PSV effect is pretty robust with PMR around or above 60% in a wide range when the Fermi energy is in the bulk band gap. This is due to the fact that the dispersive edge states in bilayer nanoribbon are nonlocalized and penetrate into the bulk, therefore it is less sensitive to the edge disorder. Experimentally, it has been found that[58] zigzag nanoribbons are more stable and easier to produce than armchair nanoribbons. All these evidences imply that the zigzag nanoribbon is a much better candidate than armchair nanoribbon for PSV application.

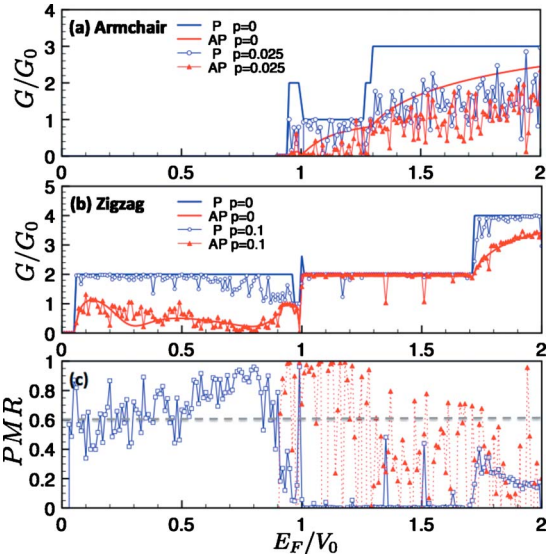

FIG. 8. (Color online) Conductance of (a) armchair ($M=80$) and (b) zigzag ($N=80$) nanoribbons with vacancies on the edge. The solid lines refer to conductance of perfect nanoribbons. The blue (red) line with hollow circle (filled triangle) refers to nanoribbons with vacancy density $p=0.1$ in zigzag or $p=0.025$ in armchair nanoribbons. In (c), the blue solid (red dashed) line with hollow square (filled triangle) refers to PMR result for zigzag (armchair) nanoribbons.

IV. CONCLUSION

In summary, we investigate the PSV effect in bilayer graphene nanoribbons. We find a midgap PSV effect exists for nanoribbons with zigzag edges, in which the PSV can operate even when the Fermi energy is in the bulk band gap. Compared to its bulk counterpart, the midgap PSV has the advantage that it can be realized with modest shifting of the Fermi energy while in the bulk PSV the Fermi energy must be shifted out of the band gap. In addition, the midgap PSV also has a wider operational range where a large on-off ratio can be consistently obtained. This effect is robust against edge disorder and the details of interface potential, making it a promising method to control the current-conducting state in graphene-based circuits at the nanoscale.

ACKNOWLEDGMENTS

We thank Yuanbo Zhang, Kirk Bevan, Tony Low, Zhengfei Wang, Shaoping Lu, and Tongcang Li for useful discussions. This work was supported by the Division of Materials Science and Engineering, Office of Basic Energy Sciences, Department of Energy, and in part by NSF (Grant No. DMR-0906025).

[1] K. S. Novoselov, A. K. Geim, S. V. Morozov, D. Jiang, Y. Zhang, S. V. Dubonos, I. V. Grigorieva, and A. A. Firsov, Science **306**, 666 (2004).

[2] A. H. Castro Neto, F. Guinea, N. M. R. Peres, K. S. Novoselov, and A. K. Geim, Rev. Mod. Phys. **81**, 109 (2009).

[3] A. K. Geim, Science **324**, 1530 (2009).

[4] A. K. Geim and K. S. Novoselov, Nat. Mater. **6**, 183 (2007).

[5] M. I. Katsnelson, Eur. Phys. J. B **51**, 157 (2006).

[6] M. I. Katsnelson, K. S. Novoselov, and A. K. Geim, Nat. Phys. **2**, 620 (2006).

[7] X. Du, I. Skachko, A. Barker, and E. Y. Andrei, Nat. Nanotechnol. **3**, 491 (2008).
[8] S. V. Morozov, K. S. Novoselov, M. I. Katsnelson, F. Schedin, D. C. Elias, J. A. Jaszczak, and A. K. Geim, Phys. Rev. Lett. **100**, 016602 (2008).
[9] K. I. Bolotin, K. J. Sikes, Z. Jiang, M. Klima, G. Fudenberg, J. Hone, P. Kim, and H. L. Stormer, Solid State Commun. **146**, 351 (2008).
[10] K. S. Novoselov, A. K. Geim, S. V. Morozov, D. Jiang, M. I. Katsnelson, I. V. Grigorieva, S. V. Dubonos, and A. A. Firsov, Nature (London) **438**, 197 (2005).
[11] Y. Zhang, Y.-W. Tan, H. L. Stormer, and P. Kim, Nature (London) **438**, 201 (2005).
[12] K. S. Novoselov, E. McCann, S. V. Morozov, V. I. Fal'ko, M. I. Katsnelson, U. Zeitler, D. Jiang, F. Schedin, and A. K. Geim, Nat. Phys. **2**, 177 (2006).
[13] E. McCann and V. I. Fal'ko, Phys. Rev. Lett. **96**, 086805 (2006).
[14] R. N. Costa Filho, G. A. Farias, and F. M. Peeters, Phys. Rev. B **76**, 193409 (2007).
[15] Y.-W. Son, M. L. Cohen, and S. G. Louie, Nature (London) **444**, 347 (2006).
[16] M. Koshino and T. Ando, Phys. Rev. B **73**, 245403 (2006).
[17] M. I. Katsnelson, Eur. Phys. J. B **52**, 151 (2006).
[18] T. Ludwig, Phys. Rev. B **75**, 195322 (2007).
[19] I. Snyman and C. W. J. Beenakker, Phys. Rev. B **75**, 045322 (2007).
[20] J. Cserti, A. Csordás, and G. Dávid, Phys. Rev. Lett. **99**, 066802 (2007).
[21] R. V. Gorbachev, F. V. Tikhonenko, A. S. Mayorov, D. W. Horsell, and A. K. Savchenko, Phys. Rev. Lett. **98**, 176805 (2007).
[22] J. Nilsson, A. H. Castro Neto, F. Guinea, and N. M. R. Peres, Phys. Rev. B **76**, 165416 (2007).
[23] J. Nilsson and A. H. Castro Neto, Phys. Rev. Lett. **98**, 126801 (2007).
[24] S. Adam and S. Das Sarma, Phys. Rev. B **77**, 115436 (2008).
[25] E. A. Henriksen, Z. Jiang, L.-C. Tung, M. E. Schwartz, M. Takita, Y.-J. Wang, P. Kim, and H. L. Stormer, Phys. Rev. Lett. **100**, 087403 (2008).
[26] B. Sahu, H. Min, A. H. MacDonald, and S. K. Banerjee, Phys. Rev. B **78**, 045404 (2008).
[27] J. Nilsson, A. H. Castro Neto, F. Guinea, and N. M. R. Peres, Phys. Rev. B **78**, 045405 (2008).
[28] I. Martin, Y. M. Blanter, and A. F. Morpurgo, Phys. Rev. Lett. **100**, 036804 (2008).
[29] D. S. L. Abergel and T. Chakraborty, Appl. Phys. Lett. **95**, 062107 (2009).
[30] D. Culcer and R. Winkler, Phys. Rev. B **79**, 165422 (2009).
[31] H. Xu, T. Heinzel, and I. V. Zozoulenko, Phys. Rev. B **80**, 045308 (2009).
[32] S. Park and H.-S. Sim, Phys. Rev. Lett. **103**, 196802 (2009).
[33] E. McCann, Phys. Rev. B **74**, 161403(R) (2006).
[34] T. Ohta, A. Bostwick, T. Seyller, K. Horn, and E. Rotenberg, Science **313**, 951 (2006).
[35] H. Min, B. Sahu, S. K. Banerjee, and A. H. MacDonald, Phys. Rev. B **75**, 155115 (2007).
[36] E. V. Castro, K. S. Novoselov, S. V. Morozov, N. M. R. Peres, J. M. B. Lopes dos Santos, J. Nilsson, F. Guinea, A. K. Geim, and A. H. Castro Neto, Phys. Rev. Lett. **99**, 216802 (2007).
[37] Y. Zhang, T.-T. Tang, C. Girit, Z. Hao, M. C. Martin, A. Zettl, M. F. Crommie, Y. R. Shen, and F. Wang, Nature (London) **459**, 820 (2009).
[38] S. H. Abedinpour, M. Polini, A. H. MacDonald, B. Tanatar, M. P. Tosi, and G. Vignale, Phys. Rev. Lett. **99**, 206802 (2007).
[39] H. Min, G. Borghi, M. Polini, and A. H. MacDonald, Phys. Rev. B **77**, 041407(R) (2008).
[40] P. San-Jose, E. Prada, E. McCann, and H. Schomerus, Phys. Rev. Lett. **102**, 247204 (2009).
[41] I. Žutić, J. Fabian, and S. Das Sarma, Rev. Mod. Phys. **76**, 323 (2004).
[42] M. Fujita, K. Wakabayashi, K. Nakada, and K. Kusakabe, J. Phys. Soc. Jpn. **65**, 1920 (1996).
[43] K. Nakada, M. Fujita, G. Dresselhaus, and M. S. Dresselhaus, Phys. Rev. B **54**, 17954 (1996).
[44] K. Wakabayashi, Phys. Rev. B **64**, 125428 (2001).
[45] W. Liu, Z. F. Wang, Q. W. Shi, J. Yang, and F. Liu, Phys. Rev. B **80**, 233405 (2009).
[46] E. V. Castro, N. M. R. Peres, J. M. B. Lopes dos Santos, A. H. Castro Neto, and F. Guinea, Phys. Rev. Lett. **100**, 026802 (2008).
[47] R. Lake, G. Klimeck, R. C. Bowen, and D. Jovanovic, J. Appl. Phys. **81**, 7845 (1997).
[48] T. Ando, Phys. Rev. B **44**, 8017 (1991).
[49] K. Wakabayashi and M. Sigrist, Phys. Rev. Lett. **84**, 3390 (2000).
[50] S. Krompiewski, J. Martinek, and J. Barnaś, Phys. Rev. B **66**, 073412 (2002).
[51] K. Wakabayashi, J. Phys. Soc. Jpn. **71**, 2500 (2002).
[52] M. Evaldsson, I. V. Zozoulenko, H. Xu, and T. Heinzel, Phys. Rev. B **78**, 161407(R) (2008).
[53] T. C. Li and S.-P. Lu, Phys. Rev. B **77**, 085408 (2008).
[54] T. Low, Phys. Rev. B **80**, 205423 (2009).
[55] T. Low and J. Appenzeller, Phys. Rev. B **80**, 155406 (2009).
[56] K. Wakabayashi, Y. Takane, M. Yamamoto, and M. Sigrist, Carbon **47**, 124 (2009).
[57] E. R. Mucciolo, A. H. Castro Neto, and C. H. Lewenkopf, Phys. Rev. B **79**, 075407 (2009).
[58] X. Jia *et al.*, Science **323**, 1701 (2009).
[59] M. P. L. Sancho, J. M. L. Sancho, and J. Rubio, J. Phys. F: Met. Phys. **14**, 1205 (1984).
[60] A. Rycerz, J. Tworzydlo, and C. W. J. Beenakker, Nat. Phys. **3**, 172 (2007).
[61] D. A. Areshkin, D. Gunlycke, and C. T. White, Nano Lett. **7**, 204 (2007).
[62] L. Chico, L. X. Benedict, S. G. Louie, and M. L. Cohen, Phys. Rev. B **54**, 2600 (1996).